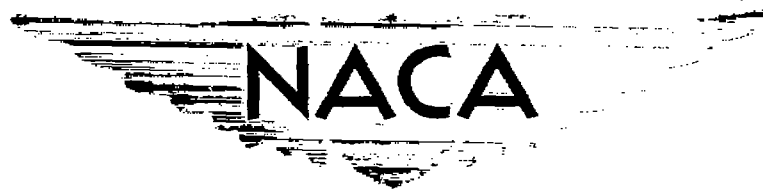


NACA RM H56E02

32



RESEARCH MEMORANDUM

LIFT AND DRAG OF THE BELL X-5 RESEARCH AIRPLANE IN THE
45° SWEPTBACK CONFIGURATION AT TRANSONIC SPEEDS

By Jack Nugent

High-Speed Flight Station
Edwards, Calif.

CLASSIFICATION CHANGED
UNCLASSIFIED

To _____
By authority of Nasa TPA 9 Effective Date 9-1-59

78 11-28-59

CLASSIFIED DOCUMENT

This material contains information affecting the National Defense of the United States within the meaning of the espionage laws, Title 18, U.S.C., Sec. 793 and 794, the transmission or revelation of which in any manner to an unauthorized person is prohibited by law.

NATIONAL ADVISORY COMMITTEE FOR AERONAUTICS

WASHINGTON

July 11, 1956

~~CONFIDENTIAL~~

UNCLASSIFIED

UNCLASSIFIED

NACA RM H56E02

NATIONAL ADVISORY COMMITTEE FOR AERONAUTICS

RESEARCH MEMORANDUM

LIFT AND DRAG OF THE BELL X-5 RESEARCH AIRPLANE IN THE
45° SWEEPBACK CONFIGURATION AT TRANSONIC SPEEDS

By Jack Nugent

SUMMARY

A flight investigation was made of the Bell X-5 variable-sweep research airplane in the 45° wing sweepback configuration over a Mach number range from 0.61 to 1.01. Lift and drag values are presented and a comparison is made with data previously obtained with a wing sweepback of 59°.

For the configuration at a wing sweep of 45° the lift-curve slope remained constant at a value of about 0.067 deg⁻¹ as Mach number increased from 0.61 to 0.80 and increased to a value of 0.078 as Mach number increased further to 0.95. Over the Mach number range tested, the configuration at 45° sweepback had a lift-curve slope approximately 0.03 deg⁻¹ higher than the slope for the 59° configuration. Below the drag rise the 45° configuration had a zero-lift drag coefficient of 0.020 as compared with a zero-lift drag coefficient of 0.0175 for the 59° sweepback configuration. The drag-rise Mach number was 0.85 for the configuration at 45° sweepback as compared to 0.90 for the wing at 59° sweepback. At 45° wing sweep the lift-drag ratio exceeded that for the 59° sweep for a Mach number range from 0.61 to 0.88 with a maximum difference of about 0.7 at a Mach number of 0.82, but was less for Mach numbers in excess of 0.88. The drag-due-to-lift factor for the 45° sweepback configuration was constant at approximately 0.18 as Mach number increased from 0.61 to 0.94. This value of drag-due-to-lift factor was about 0.12 less than that for the 59° sweepback configuration.

INTRODUCTION

The NACA High-Speed Flight Station has conducted flight tests with the Bell X-5 variable-sweep research airplane in the transonic speed range as a part of the joint Air Force-Navy-NACA high-speed flight research program. The wing sweep of the airplane is variable in flight from 20° to 59°. The lift and drag characteristics of the 59° sweepback configuration have been measured over the Mach number range from 0.6 to 1.03

UNCLASSIFIED

and reported in reference 1, and a small amount of data for the 20° swept-back configuration is also included in reference 1. This paper presents the lift and drag characteristics of the airplane with a 45° sweepback and makes a comparison with unpublished data for the 59° sweptback configuration. These unpublished data are similar to those of reference 1, but were actually obtained later during more extensive flights with improved instrumentation. The data for the configuration at 45° sweepback cover the Mach number range from 0.72 to 1.01 and the usable lift range of the airplane. The present data were obtained with power on during several push-down-pull-up maneuvers and accelerated turns, as well as one speed run through a Mach number range from 0.72 to 1.01. The flights were made at Edwards, Calif.

SYMBOLS

A	aspect ratio
A _d	inlet duct area at pressure-measuring station, sq ft
A _e	exit area of jet nozzle measured cold, sq ft
a _n	measured normal acceleration, g units
a _x	measured longitudinal acceleration, g units
C _D	airplane drag coefficient
C _F	jet nozzle coefficient
C _L	airplane lift coefficient
C _{L_α}	slope of lift curve, deg ⁻¹
C _N	airplane normal-force coefficient
C _X	longitudinal-force coefficient
$\frac{dC_D}{dC_L^2}$	drag-due-to-lift factor
F _g	gross thrust, lb

F_n	net thrust, $F_g - F_r$, lb
F_r	ram drag, lb
g	acceleration due to gravity, ft/sec ²
h_p	pressure altitude, ft
$\left(\frac{L}{D}\right)_{\max}$	maximum value of lift-drag ratio
M	airplane Mach number
M_D	inlet duct Mach number at pressure-measuring station
p_a	ambient static pressure, lb/sq ft
p_d	inlet duct static pressure at pressure-measuring station, lb/sq ft
p'_e	total pressure at jet nozzle exit, lb/sq ft
q	free-stream dynamic pressure, lb/sq ft
S	wing area, sq ft
W	airplane weight, lb
α	angle of attack of airplane center line, deg
Λ	angle of sweep, deg

AIRPLANE

The Bell X-5 research airplane is a transonic research vehicle with wing sweepback variable in flight between 20° and 59°. Present tests were made with the wing at 45° sweepback, with the trailing edge of the wing at the wing root faired in to avoid the sharp discontinuity in wing section that had previously existed for all sweep angles less than 59°.

A photograph of the Bell X-5 airplane with the wing at the 45° swept-back position is given in figure 1 and a three-view drawing is presented in figure 2. The physical characteristics of the airplane are given in table I. Table II compares several pertinent wing constants for the 45°

and 59° sweep configurations. The wing slats were locked in the fully retracted position for all tests reported in this paper. The powerplant is an axial-flow turbojet engine, nonafterburning, with fixed area jet nozzle.

INSTRUMENTATION

Standard NACA recording instruments were installed in the airplane to measure the following pertinent quantities:

- Airspeed
- Altitude
- Normal acceleration
- Longitudinal acceleration
- Angle of attack
- Inlet duct static and total pressure
- Jet nozzle exit total pressure

All the instruments were synchronized by a common timer.

Altitude and airspeed were determined by an NACA airspeed head mounted on the nose boom, and angle of attack was measured by a vane attached to an arm projecting from the nose boom. The vane is approximately 50 inches ahead of the nose fairing and 7 inches to the left of the center line of the boom. Total pressures in the inlet duct and tailpipe were measured with cantilever-type probes inserted into the gas stream, whereas static pressure was measured with flush orifices attached to the duct wall.

THRUST AND DRAG DETERMINATION

Gross thrust and ram drag were determined in flight by measuring inlet duct total and static pressure, exit nozzle total pressure, and ambient pressure. For all the flight tests reported in this paper, sonic flow was established at the jet nozzle exit permitting use of the following equation for gross thrust (ref. 2):

$$F_g = C_f A_e (1.259 p'_e - p_a)$$

The value of C_f was determined from ground runs on a thrust stand. A value of 0.948 was the measured value for the tests reported. Ram drag was determined from the following equation:

$$F_r = 1.4 p_d A_d M_D \sqrt{\frac{1 + 0.2 M_D^2}{1 + 0.2 M^2}}$$

Local Mach number in the duct was determined from measurements of total and static pressure.

The lift and drag coefficients were computed using the following formulas:

$$C_N = \frac{W a_n}{q S}$$

$$C_X = \frac{F_n - W a_x}{q S}$$

$$C_L = C_N \cos \alpha - C_X \sin \alpha$$

$$C_D = C_X \cos \alpha + C_N \sin \alpha$$

ACCURACY

The following accuracies of measurement are felt to be applicable for the results presented:

α (overall average), deg	± 0.5
a_n , g	± 0.05
a_x , g	± 0.005
F_n , lb	± 75
M (maximum)	± 0.01
q at $M = 0.8$ and $h_p = 37,500$ ft ($\Delta p_a = 4.41$ lb/sq ft,	
$\Delta M = 0.01$), lb/sq ft	± 3.0
W , lb	± 25

The nonobservational errors associated with the angle-of-attack measurement are floating angle of the vane, upwash over the airplane and nose boom, pitching velocity effects, and bending of the nose boom. The effects of vane floating were measured by flying the airplane at similar flight conditions with the nose boom rotated 180° from its normal position. A preliminary investigation was made of the latter three effects on the angle-of-attack measurement for the 59° sweptback configuration using a sun camera and sensitive differential pressure recorders and accelerometers. The results of this preliminary investigation did

not cover sufficient range to permit a correction, but indicated that the stated values of angle of attack are accurate to $\pm 0.25^\circ$ at low-lift coefficients and to $\pm 0.50^\circ$ at high-lift coefficients.

The error in C_L was 5 percent or less throughout most of the lift range presented. The accuracy of the drag coefficient depends primarily on the accuracies of thrust, angle of attack, longitudinal acceleration, normal acceleration, weight, and Mach number. By using the maximum estimated errors in these quantities individually, a drag coefficient error was calculated for a range of dynamic pressures encountered in flight. The values of drag coefficient error for individual data points varied from 0.0039 to 0.0013, excluding the effects of angle of attack. Fairing the data eliminates many of the random errors and it is felt that the drag coefficient curves are within ± 0.0010 at the lower values of lift coefficient.

TESTS, RESULTS, AND DISCUSSION

Lift and drag were determined for the Bell X-5 research airplane in the 45° wing sweepback configuration in the clean condition. Data were obtained over an altitude range from about 35,000 to about 41,000 feet during several push-down—pull-up maneuvers and accelerated turns, and one level run. Reynolds number based on the wing mean aerodynamic chord varied from 8×10^6 to 18×10^6 for a Mach number range of 0.61 to 1.01. The elevator alone was used during turns and pull-ups since stabilizer position was fixed for a particular maneuver. Stabilizer position varied from 3.7° trailing edge up to 3.1° trailing edge up; elevator position varied from 12.1° trailing edge up to 4.3° trailing edge down, for the data presented.

Figure 3 presents the variation of lift coefficient with angle of attack for several Mach numbers. Each curve presents data covering a narrow band of Mach number about the stated Mach number. Below the drag-rise Mach number the band was ± 0.025 and at higher Mach numbers it was reduced to ± 0.005 . There was a general tendency for the curves to be linear up to a lift coefficient of 0.5. Straight lines were faired to those portions of the curves between lift coefficient values of 0 and 0.5 and were extended to zero lift when feasible. The angle of attack for zero lift decreased slightly from about 1° at a Mach number of 0.71 to about 0.5° at a Mach number of 0.96.

The slopes of the lift curves for those portions between lift coefficient values of 0 and 0.5 are plotted against Mach number in figure 4. Also shown are data for the 59° sweptback configuration, which differ from the data of reference 1, as explained in the INTRODUCTION. The lift-curve slope for the 45° configuration had a relatively constant value of

approximately 0.067 deg^{-1} for a Mach number range of 0.6 to 0.8, then rose gradually to a value of about 0.078 deg^{-1} as Mach number increased from 0.8 to 0.96. Over the Mach number range from 0.6 to 0.96 the lift-curve slope for the 45° configuration exceeded that for the 59° configuration by about 0.03 deg^{-1} .

Figure 5 presents the variation of lift coefficient with drag coefficient for several Mach numbers.

Figure 6 presents the variation of drag coefficient with Mach number for constant values of lift coefficient. Drag levels were selected from the drag data of figure 5 at lift coefficient values of 0.2, 0.3, 0.4, and 0.5, when possible. Extrapolated values at zero lift were also obtained.

As Mach number increased from 0.71 to 0.84, the zero-lift drag coefficient remained sensibly constant at 0.020; at the higher values of lift coefficient there was also little effect of Mach number on drag coefficient. The drag-rise Mach number, defined as the point at which the slope of drag coefficient with Mach number equals 0.1, decreased slightly from a value of 0.88 at zero lift as lift coefficient increased to 0.5.

A comparison is made in figure 7 of the variation of drag coefficient with Mach number for the 45° and 59° configurations at lift coefficients of 0 and 0.2. At zero lift, sweeping the wings to 59° increased the drag-rise Mach number from 0.88 to 0.91 and decreased the drag coefficient by about 0.0025 for a Mach number range from 0.71 to 0.84. At 0.2 lift coefficient, sweeping the wings to 59° increased the drag-rise Mach number from about 0.87 to 0.92 and reduced the drag coefficient by about 0.012 at a Mach number of 0.94.

The variation of the maximum lift-drag ratio with Mach number is presented in figure 8 for the 45° and 59° configurations. For the 45° configuration the curve was relatively constant at about 8.7 for the Mach number range from 0.61 to 0.74, rose to a peak value of about 9.1 at a Mach number of 0.81, and decreased sharply as Mach number increased above 0.86. The lift-drag ratio for the 45° configuration exceeded that for the 59° configuration for a Mach number range from 0.61 to 0.88 with a maximum difference of about 0.7 at a Mach number of 0.82, but was less for Mach numbers in excess of 0.88.

Figure 9 presents the variation of C_L for $\left(\frac{L}{D}\right)_{\max}$ against Mach number and also the altitude required for level flight at maximum lift-drag ratio for the 45° configuration. The latter curve increased steadily from a value of 35,000 feet at a Mach number of 0.7 to 50,000 feet at a Mach number of about 0.93.

Figure 10 presents the data of figure 5 plotted as drag coefficient against lift coefficient squared. Straight lines were faired to those portions of the curves between lift coefficient values slightly above 0 and 0.4. The slopes of the straight lines thus obtained are a measure of the drag-due-to-lift for the lift-coefficient range cited. The magnitude of the slopes depends on the lift-coefficient range selected for fairing because of the increase of drag-due-to-lift factor with lift coefficient.

Figure 11 presents the variation of drag-due-to-lift factor with Mach number along with the theoretical limits $\frac{1}{\pi A}$ and $\frac{1}{C_{L\alpha}}$ for 100 percent and zero leading-edge suction, respectively. Also shown is the variation of drag-due-to-lift factor for the 59° configuration for a C_L range from about 0 to 0.4. The value of drag-due-to-lift factor for the 45° configuration remained constant at approximately 0.18 for a Mach number range from 0.61 to 0.94. This value of drag-due-to-lift factor was about 0.12 less than that for the 59° sweptback configuration. The theoretical curves indicate that at the lower Mach numbers about half the possible leading-edge suction was achieved by the 45° configuration.

CONCLUSIONS

Lift and drag measurements obtained in flights with the Bell X-5 variable-sweep research airplane in the 45° sweptback configuration for a Mach number range from 0.61 to 1.01, and a comparison with comparable data obtained in the 59° sweptback configuration, led to the following conclusions:

1. In the 45° configuration the lift-curve slope remained constant at a value of approximately 0.067 deg⁻¹ as Mach number increased from 0.61 to 0.80, and increased to a value of 0.078 as Mach number further increased to 0.96. Over the Mach number range tested the 45° sweptback configuration had a lift-curve slope about 0.03 deg⁻¹ higher than the slope for the 59° configuration.
2. Below the drag rise the 45° configuration had a zero-lift drag coefficient of 0.020 as compared with 0.0175 for the 59° sweptback configuration. The zero-lift drag-rise Mach number was 0.88 for the 45° sweptback configuration as compared to 0.91 for the 59° sweptback configuration.
3. The lift-drag ratio for the configuration at 45° sweep exceeded that for the 59° configuration for a Mach number range from 0.61 to 0.88 and was less for Mach numbers in excess of 0.88. A maximum difference of about 0.7 occurred at a Mach number of 0.82.

4. The drag-due-to-lift factor for the 45° sweptback configuration was constant at approximately 0.18 as Mach number increased from 0.61 to 0.94. This value of drag-due-to-lift factor was about 0.12 less than that for the 59° sweptback configuration.

High-Speed Flight Station,
National Advisory Committee for Aeronautics,
Edwards, Calif., April 13, 1956.

REFERENCES

1. Bellman, Donald R.: Lift and Drag Characteristics of the Bell X-5 Research Airplane at 59° Sweepback for Mach Numbers From 0.60 to 1.03. NACA RM L53A09c, 1953.
2. Fleming, William A., and Gabriel, David S.: A Survey of Methods for Turbojet Thrust Measurement Applicable to Flight Installations. NACA RM E55D05a, 1955.

TABLE I

PHYSICAL CHARACTERISTICS OF BELL X-5 AIRPLANE AT 45° SWEEPBACK

Airplane:

Weight, lb:

Full fuel	10,006
Less fuel	7,894

Powerplant:

Axial-flow turbojet engine	J35-A-17
Guaranteed rated thrust at 7,800 rpm and static sea-level conditions, lb	4,900

Center-of-gravity position, percent mean aerodynamic chord:

Sweep angle, deg	45
Full fuel	45.0
Less fuel	45.5
Overall height, ft	12.2
Overall length, ft	33.6

Moment of inertia about Y-axis, slug-ft²:

Full fuel	9,495
Less fuel	8,040

Wing:

Airfoil section (perpendicular to 38.02 percent chord line):

Pivot point	NACA 64(10)A011
Tip	NACA 64(08)A008.28
Sweep angle at 25 percent chord, deg	45
Area, sq ft	172.2
Span, ft	24.76
Span between equivalent tips, ft	24.56
Aspect ratio	3.56
Taper ratio	0.4398
Mean aerodynamic chord, ft	7.72
Location of leading edge of mean aerodynamic chord, fuselage station	126.4
Incidence root chord, deg	0
Dihedral, deg	0
Geometric twist, deg	0

Wing flaps (split):

Area, sq ft	15.9
Span, parallel to hinge center line, ft	6.53
Chord, parallel to line of symmetry at 20° sweepback, in.:	
Root	30.8
Tip	19.2
Travel, deg	60

Slats (leading edge divided):

Area, sq ft	14.6
Span, parallel to leading edge, ft	10.3
Chord, perpendicular to leading edge, in.:	
Root	11.1
Tip	6.6

Travel, percent wing chord:

Forward	10
Down	5

Aileron (45 percent internal-seal pressure balance):

Area (each aileron behind hinge line), sq ft	3.62
Span parallel to hinge center line, ft	5.15
Travel, deg	±15
Chord, percent wing chord	19.7
Moment area rearward of hinge line (total), in. ³	4,380

TABLE I.- Concluded

PHYSICAL CHARACTERISTICS OF BELL X-5 AIRPLANE AT 45° SWEEPBACK

Horizontal tail:

Airfoil section (parallel to fuselage center line)	NACA 65A006
Area (including area covered by fuselage), sq ft	31.5
Span, ft	9.56
Aspect ratio	2.9
Taper ratio	0.371
Sweep angle at 25 percent chord, deg	45
Mean aerodynamic chord, in.	42.8
Position of 25 percent mean aerodynamic chord, fuselage station	355.6
Stabilizer travel (power actuated), deg:	
Leading edge up	4.5
Leading edge down	7.5
Elevator (20.8 percent overhang balance, 31.5 percent elevator span):	
Area rearward of hinge line, sq ft	6.9
Travel from stabilizer, deg:	
Up	25
Down	20
Chord, percent horizontal tail chord	30
Moment area rearward of hinge line (total), in. ³	4,200

Vertical tail:

Airfoil section (parallel to rear fuselage center line)	NACA 65A006
Area (above rear fuselage center line), sq ft	25.8
Span, perpendicular to rear fuselage center line, ft	6.17
Aspect ratio	1.47
Sweep angle of leading edge, deg	46.6
Fin:	
Area, sq ft	24.8
Rudder (25.1 percent overhang balance, 26.3 percent middle span):	
Area rearward of hinge line, sq ft	4.7
Span, ft	4.43
Travel, deg	±35
Chord, percent horizontal-tail chord	22.7
Moment area rearward of hinge line, in. ³	3,585

TABLE II

PERTINENT WING CHARACTERISTICS FOR THE 45°
AND 59° SWEPTBACK CONFIGURATIONS

	Sweep angle, deg (at 25 percent chord) 45°	Sweep angle, deg (at 25 percent chord) 59°
Area, sq ft	172.2	184.3
Aspect ratio	3.56	2.16
Streamwise thickness, percent chord:		
Root	7.9	6.9
Tip	6.3	4.7



E-812

Figure 1.- Photograph of Bell X-5 research airplane at 45° sweepback.

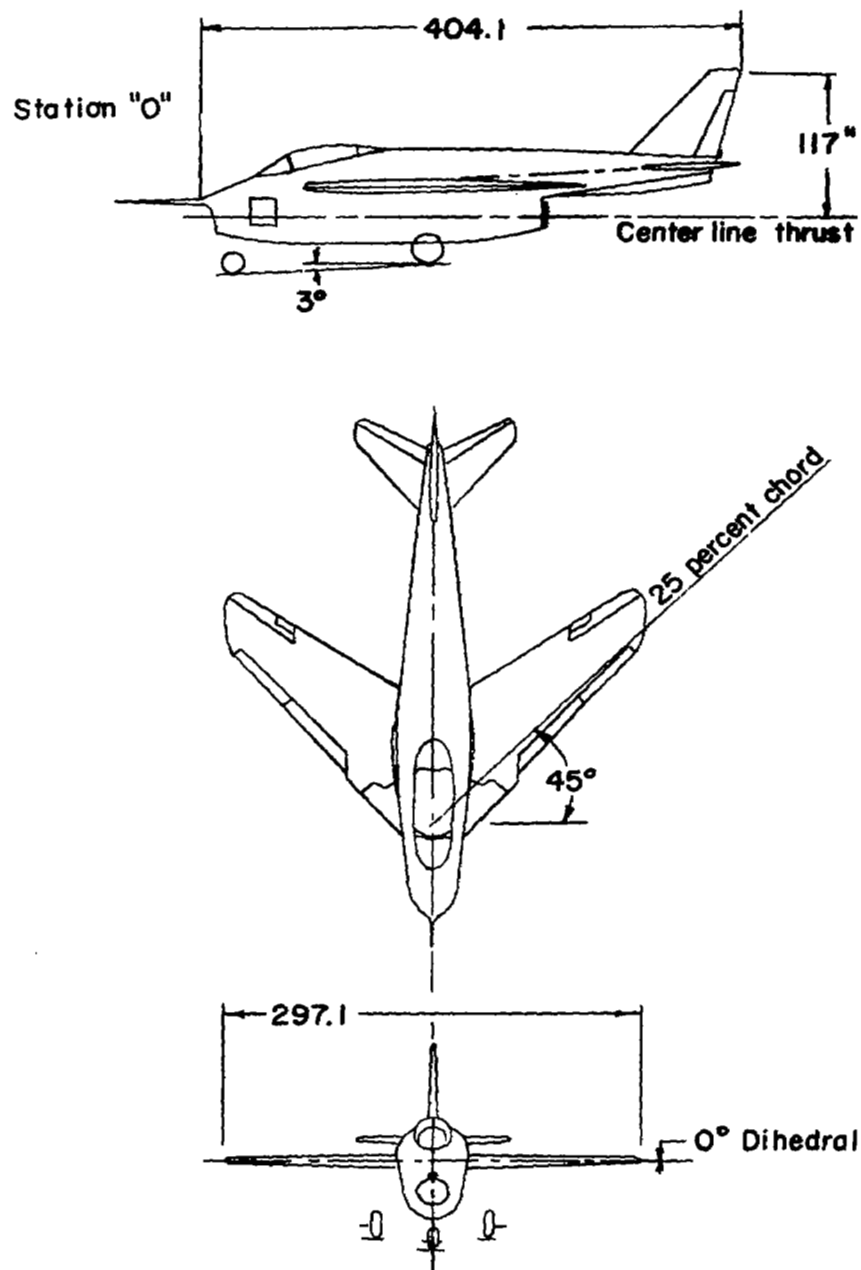


Figure 2.- Three-view drawing of Bell X-5 research airplane at 45° sweepback.

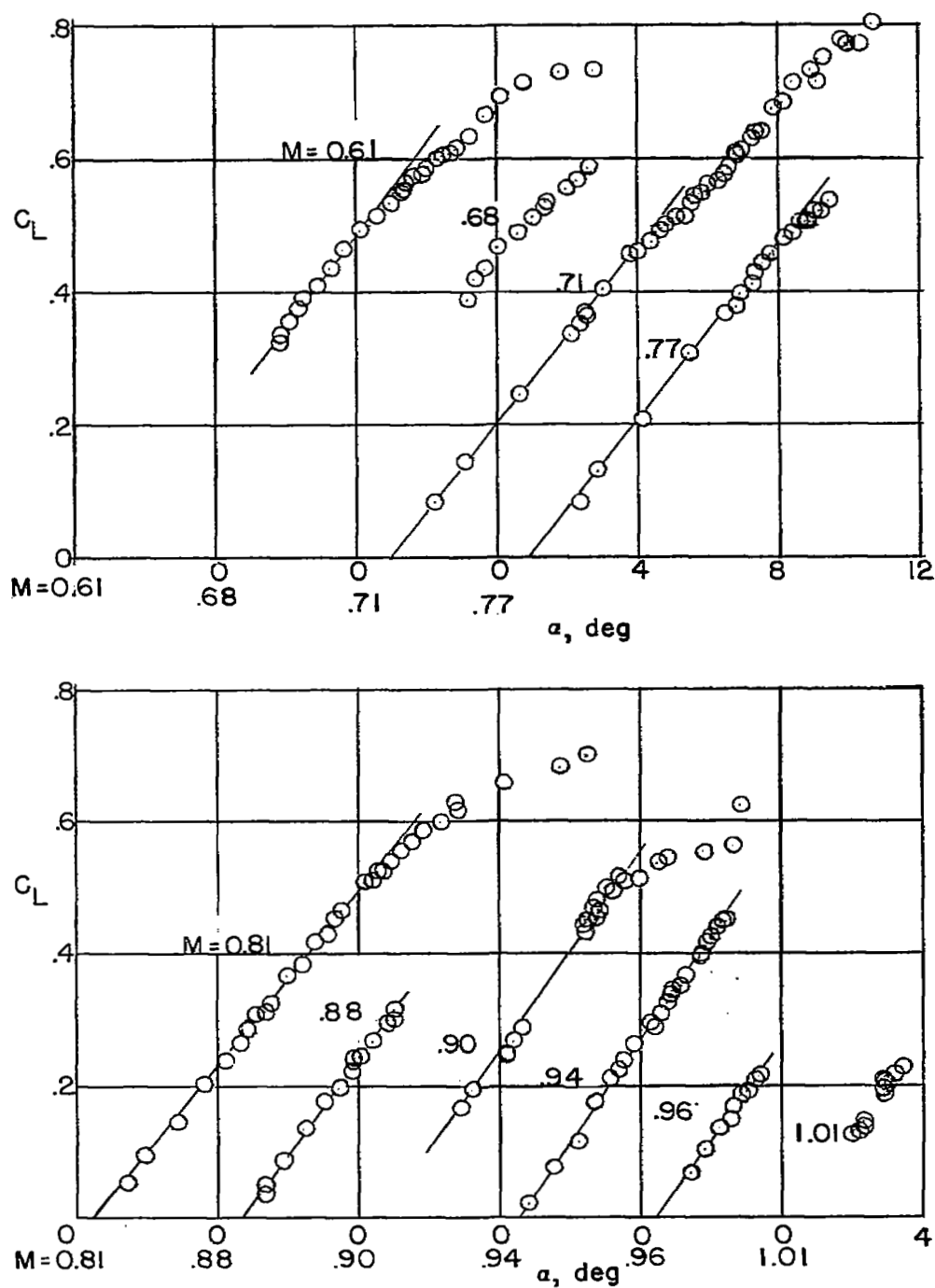


Figure 3.- Variation of lift coefficient with angle of attack for several Mach numbers.

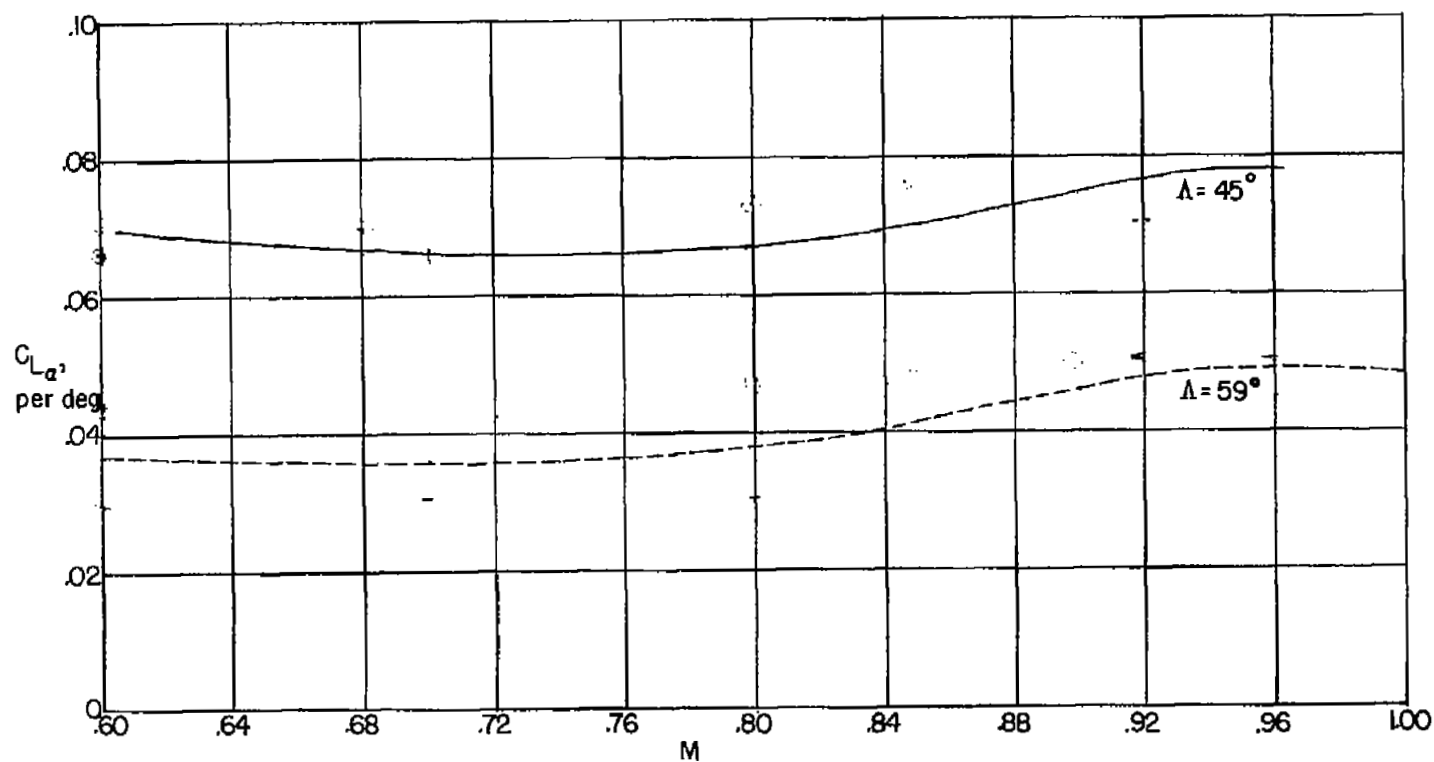


Figure 4.- Variation of lift-curve slope with Mach number.

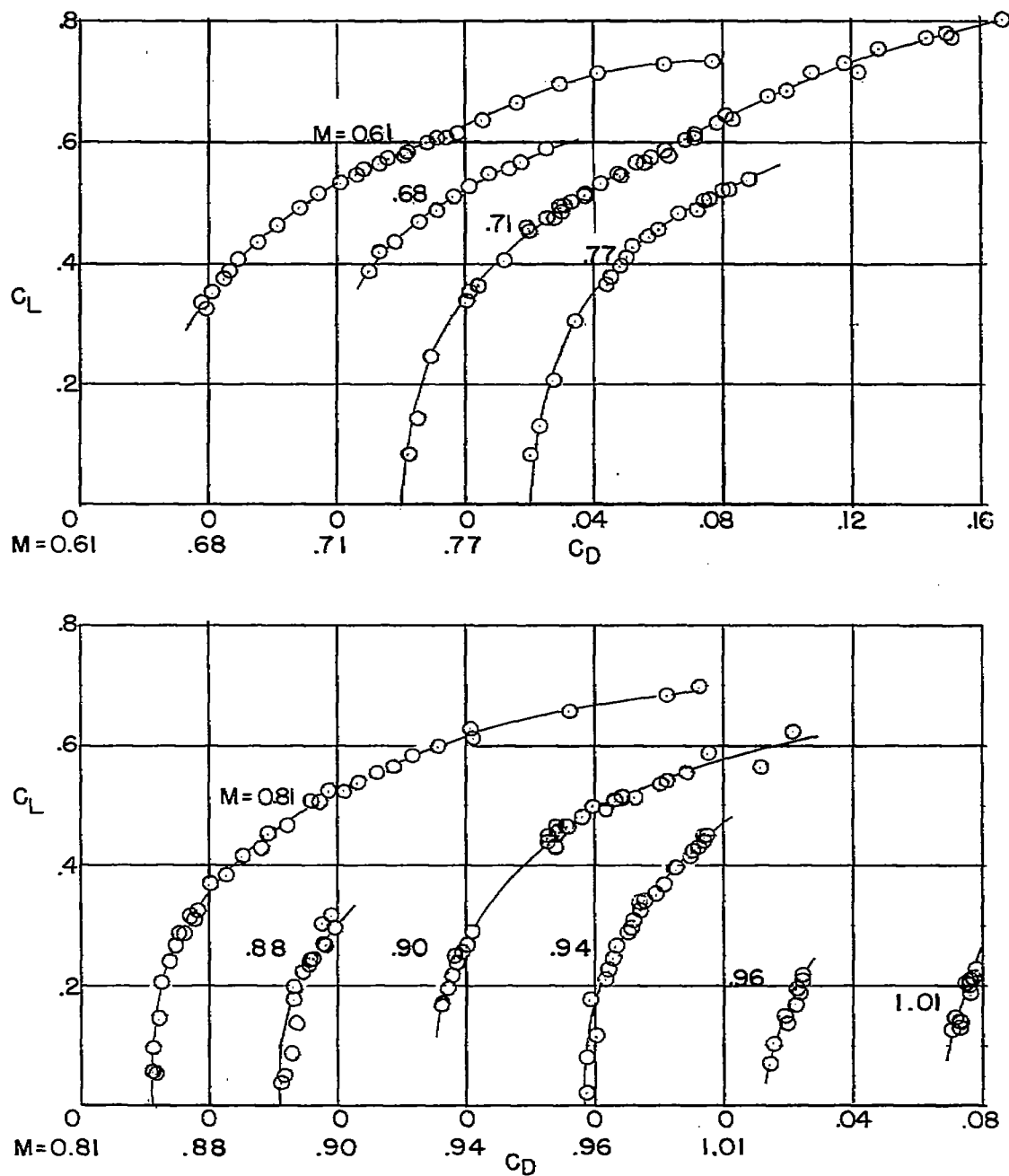


Figure 5.- Variation of lift coefficient with drag coefficient for several Mach numbers.

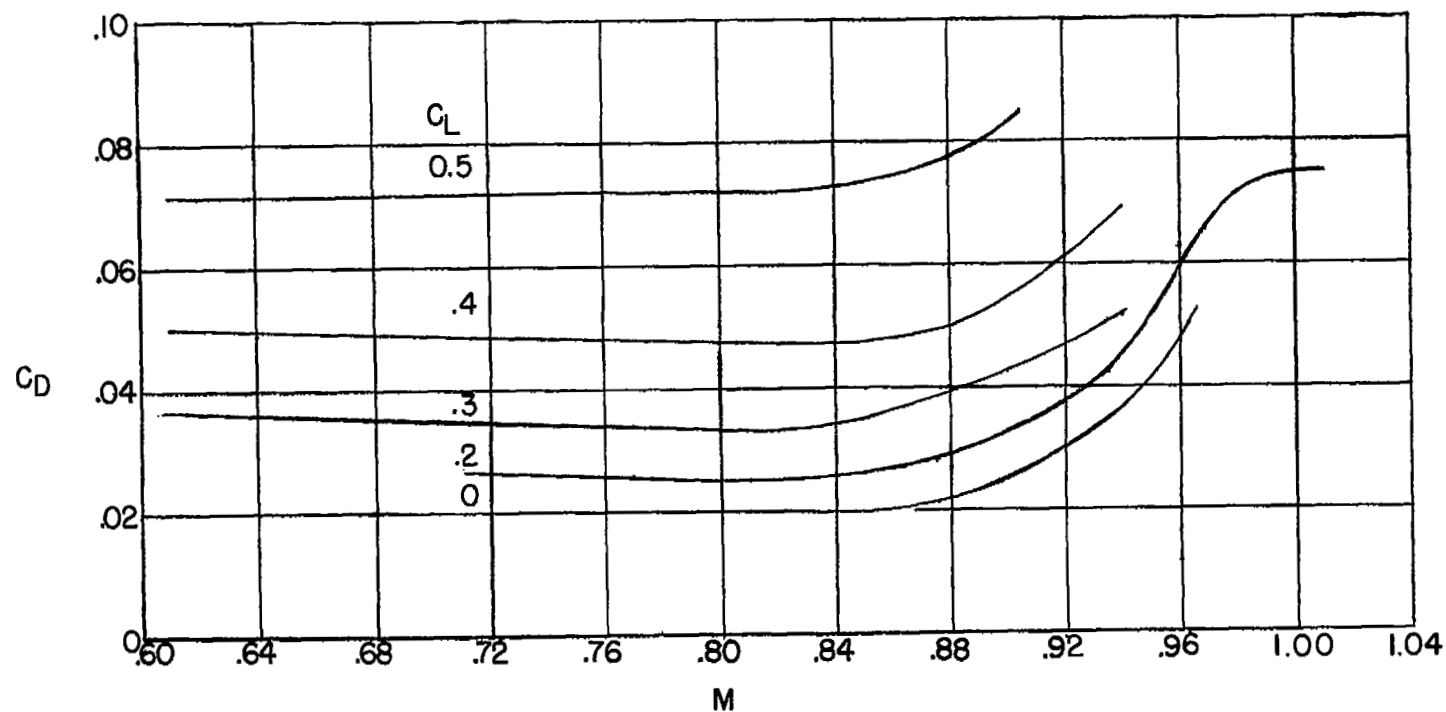


Figure 6.- Variation of drag coefficient with Mach number for several lift coefficients. (45° configuration.)

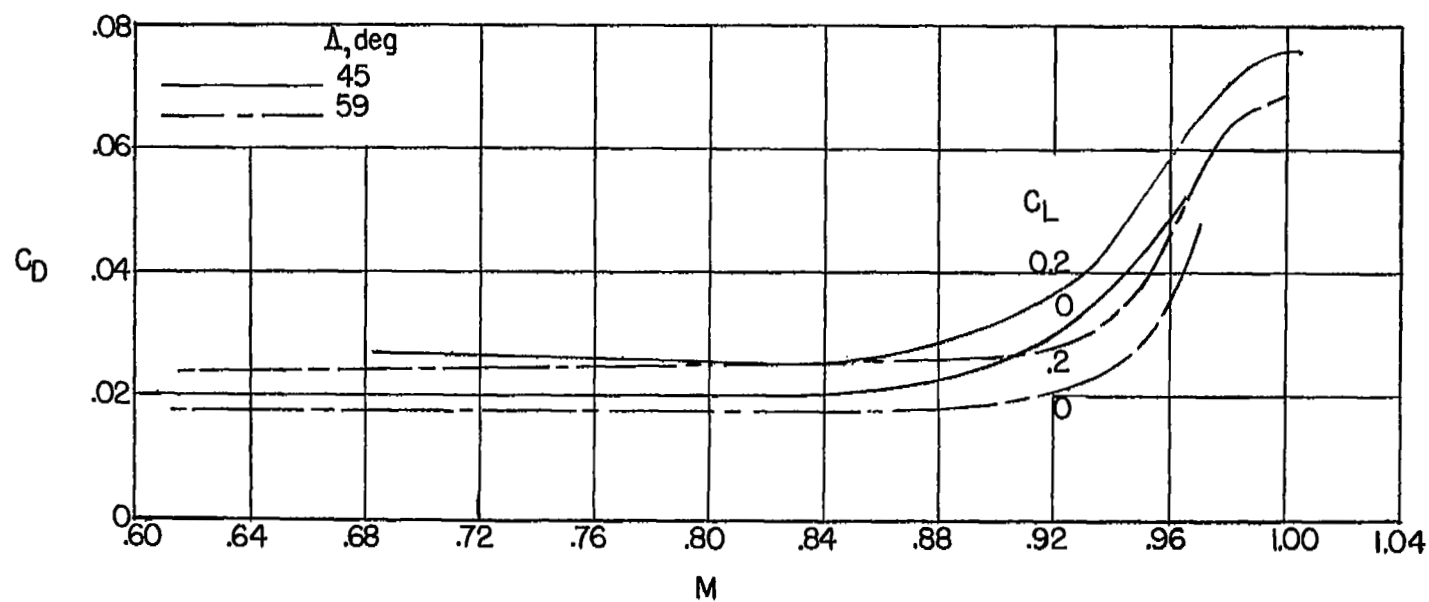


Figure 7.- Drag coefficient variation with Mach number for the 45° and 59° configurations.

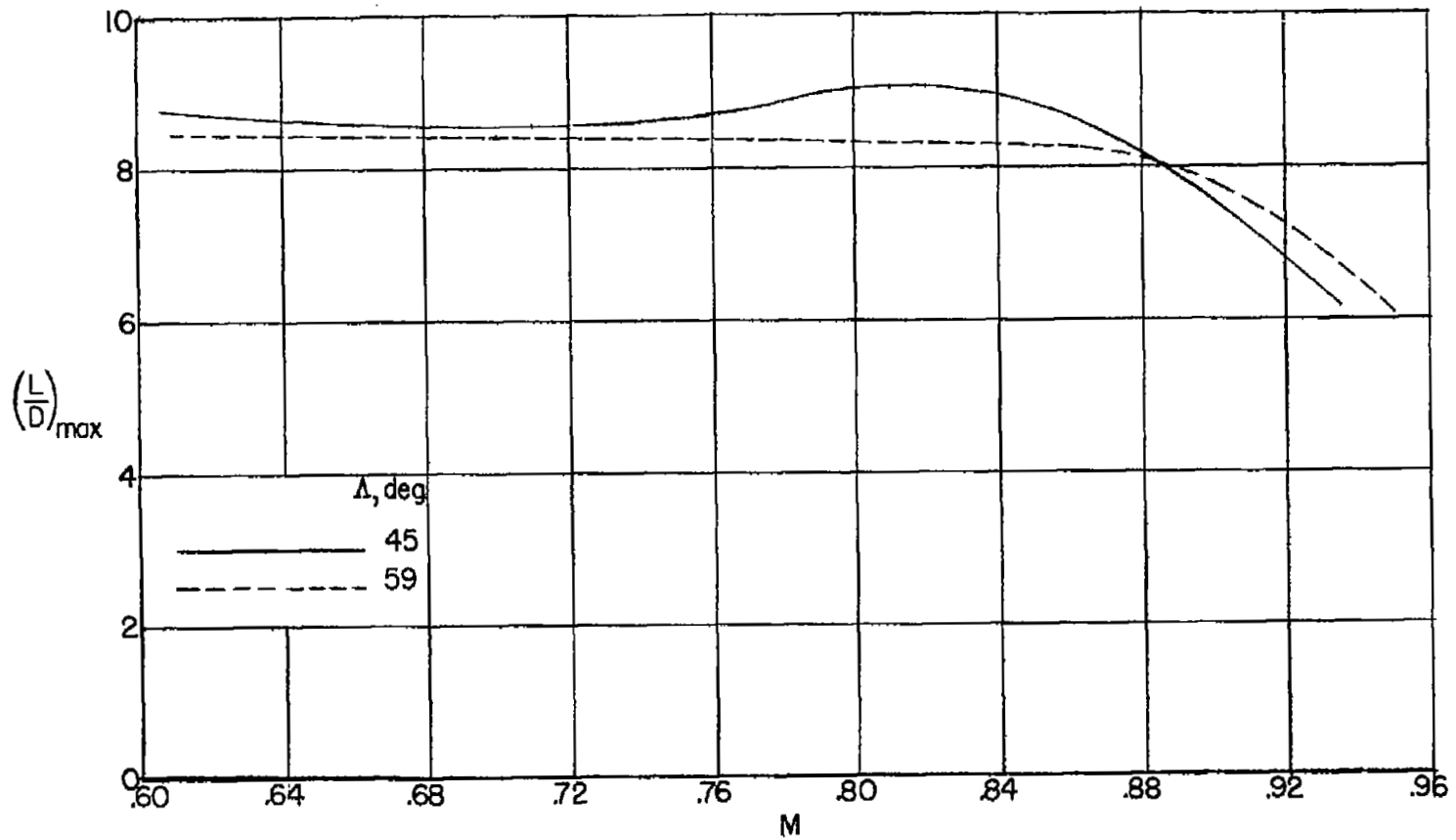


Figure 8.- Variation of $(L/D)_{\max}$ with Mach number.

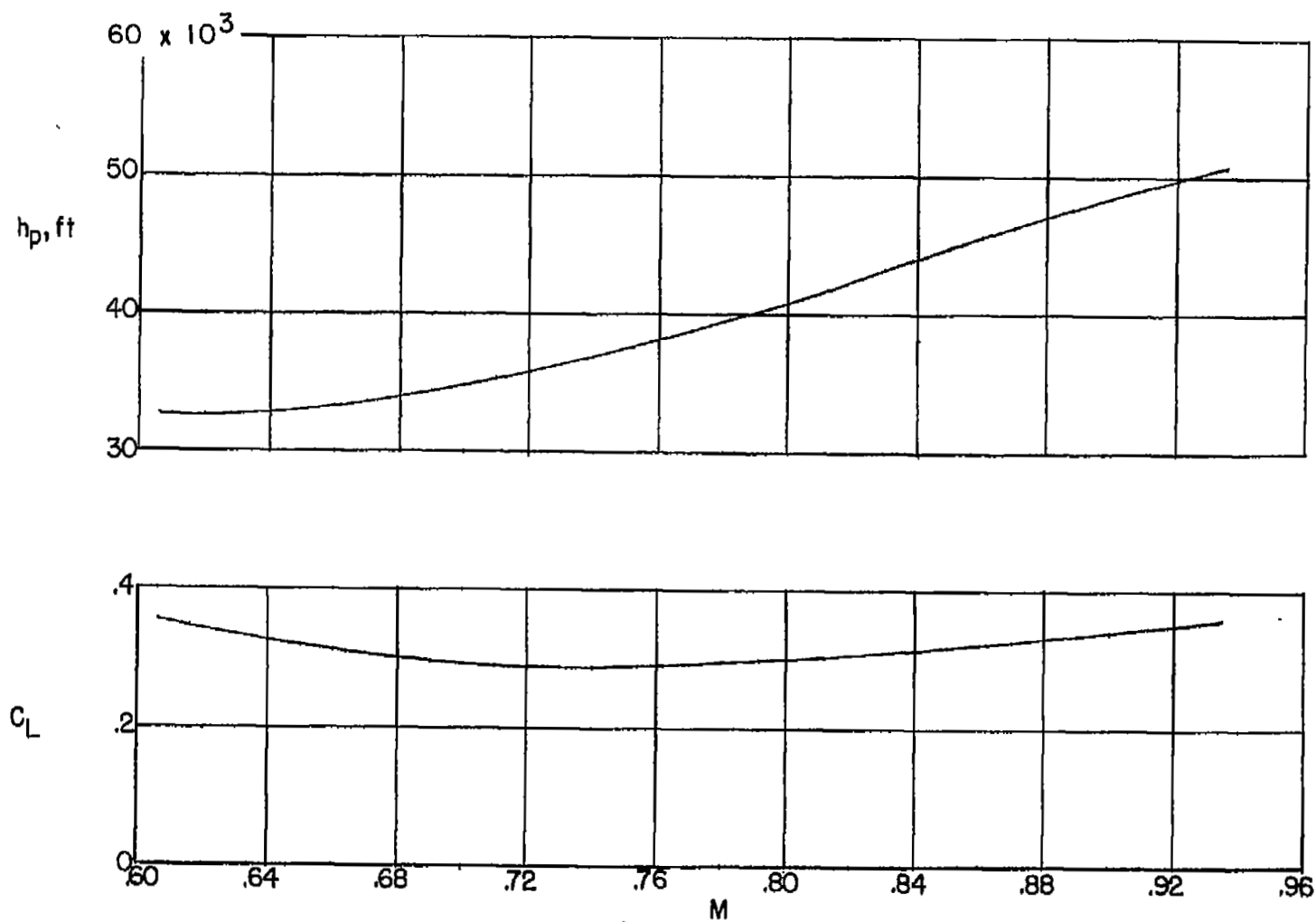


Figure 9.- Variation of C_L for $(L/D)_{\max}$ and level flight altitude for $(L/D)_{\max}$ with Mach number.

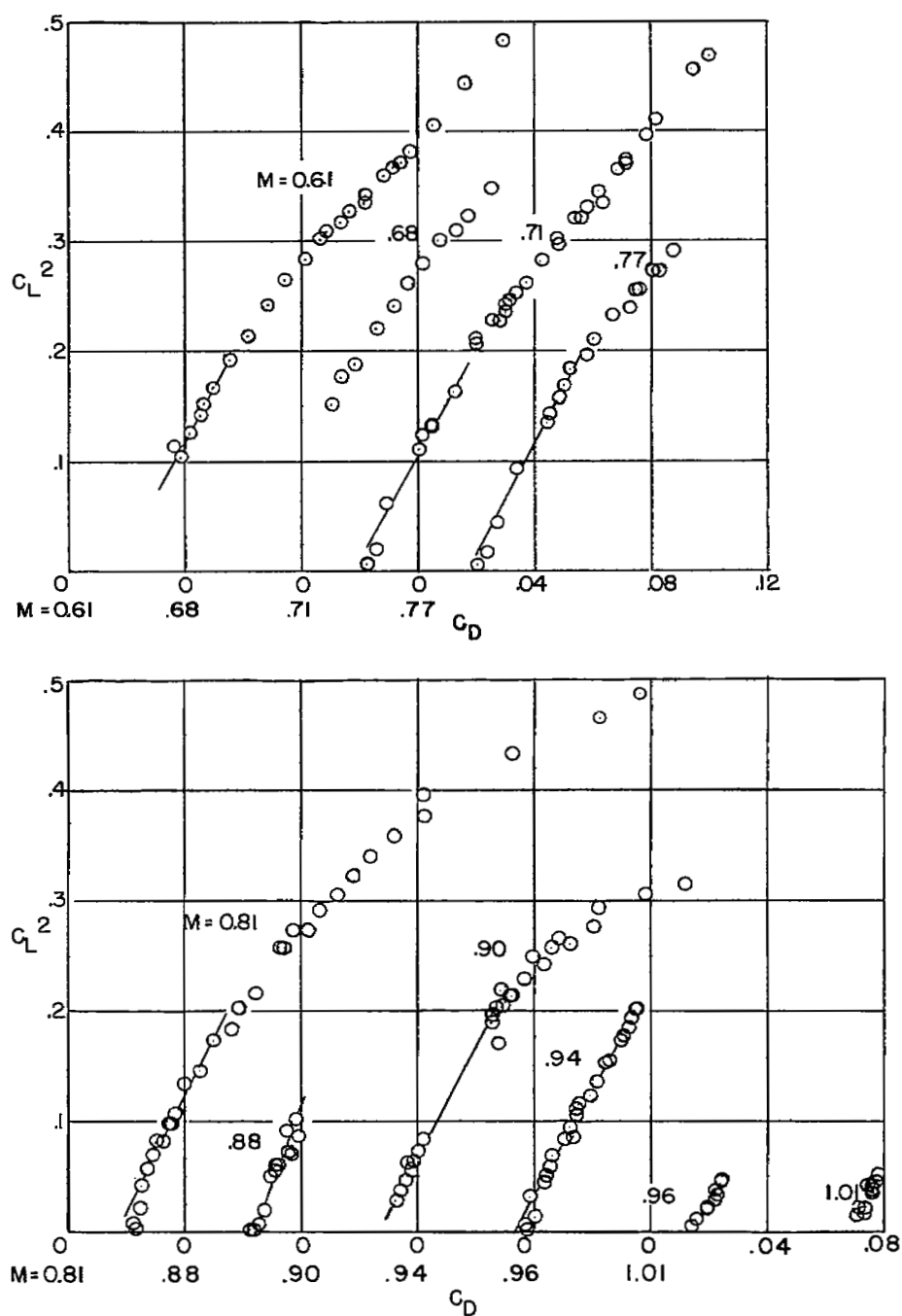


Figure 10.- Variation of drag coefficient with lift coefficient squared for several Mach numbers.

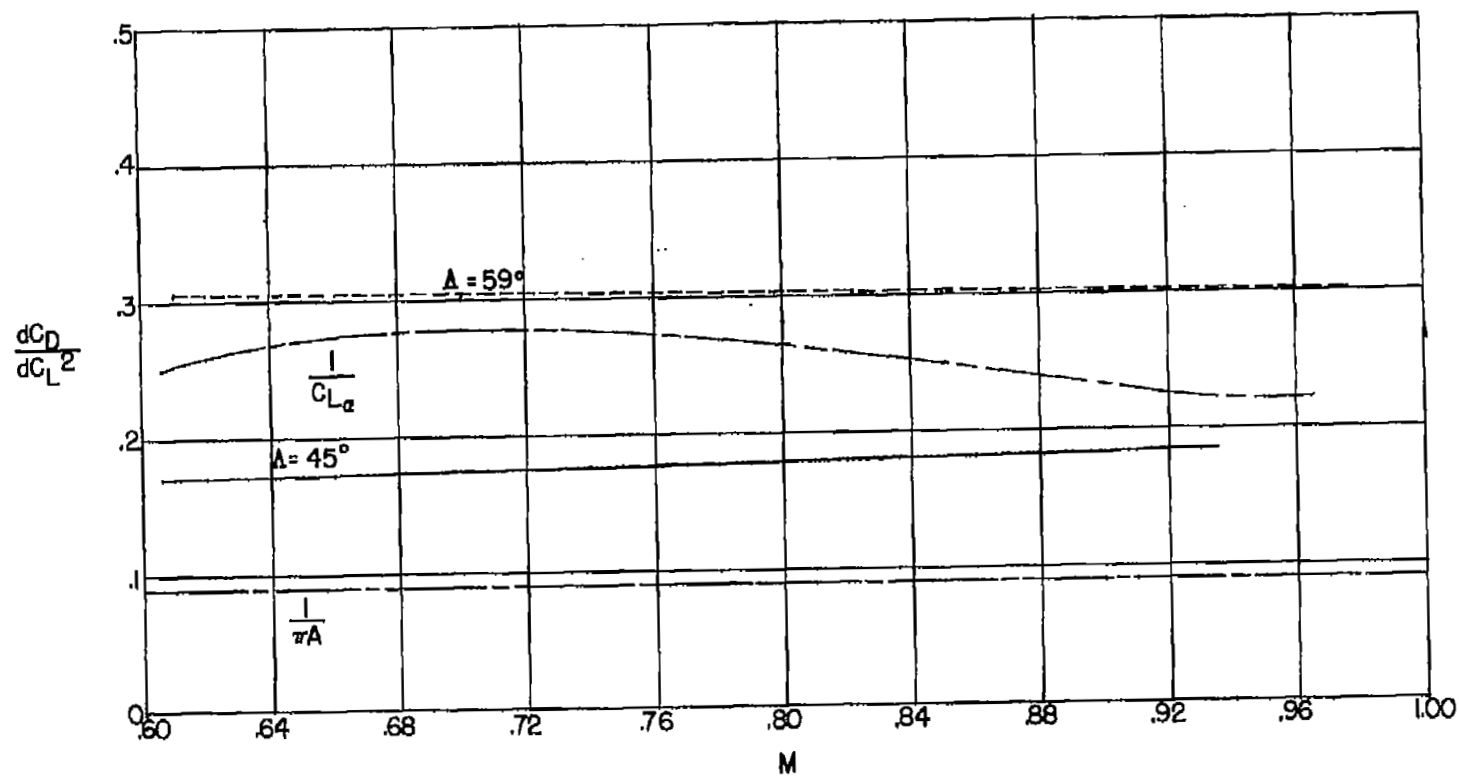


Figure 11.- Variation of drag-due-to-lift factor with Mach number.